State of Charge Estimation for Lithium-Ion Batteries in Hybrid Vessels Using Kalman Filters

Author(s): Elsanhoury, Mahmoud; Koljonen, Janne; Elmusrati, Mohammed; Niemi, Seppo

Title: State of Charge Estimation for Lithium-Ion Batteries in Hybrid Vessels Using Kalman Filters

Year: 2025

Version: Accepted manuscript

State of Charge Estimation for Lithium-Ion Batteries in Hybrid Vessels Using Kalman Filters

Mahmoud Elsanhoury
Digital Economy Platform
University of Vaasa
Vaasa, Finland
first.lastname@uwasa.fi

Janne Koljonen
Automation Technology
University of Vaasa
Vaasa, Finland
first.lastname@uwasa.fi

Mohammed Elmusrati
Telecommunications Engineering
University of Vaasa
Vaasa, Finland
first.lastname@uwasa.fi

Seppo Niemi
Energy Technology
University of Vaasa
Vaasa, Finland
first.lastname@uwasa.fi

***Abstract*—Lithium-ion (Li-ion) batteries have gained significant attention in applications such as electric vehicles and hybrid vehicles and vessels. An important variable of the battery pack is the state-of-charge (SoC), which is not deterministic and cannot be measured accurately using the currently available methods, but it requires estimation. The Kalman filter algorithm has proven to be reliable in estimating the charging level of Li-ion batteries. In this paper, we compare the performance of two different Kalman-based algorithms in terms of robustness and accuracy, also distinct in the nonlinearity scheme. A polynomial curve fitting method is customized to estimate the essential Li-ion battery parameters based on its Thevenin equivalent circuit model. Then, the output of these parameter estimations is propagated through two Kalman filters: extended Kalman filter (EKF) and the unscented Kalman filter (UKF). The implemented filter algorithms are validated using realistic data collected from a functional hybrid vessel operating between the Nordic countries. Further validation for the battery parameters is done using laboratory experiments on battery packs. The SoC estimation results show that both filters EKF and UKF converge robustly and reliably. However, UKF is further recommended as it outperforms EKF in terms of battery SoC estimation accuracy with an advantage of 0.05% error, hence, making UKF more suitable for real-time Li-ion battery-based applications.**

***Index Terms*—State of charge estimation, Kalman filters, Lithium-ion, Battery, Hybrid vessels.**

I. Introduction

A. Role of batteries in hybrid maritime shipping

Hybrid vessels (ships) are designed to minimize emissions by optimally utilizing several power sources, e.g., main and auxiliary internal combustion engines (ICE), and electric generators/motors (G/M). These power sources are connected to a powertrain as shown in Figure 1. The Power Take In Power Take Out (PTIPTO) unit controls the power flow direction of the G/M: energy stored in the battery can be used to support the ICE to drive propulsion or energy generated by the ICE can be stored to the battery. The objective of the hybrid drive control is to enable using the ICE as efficiently as possible and with minimized emissions. The role of the electric powertrain is, e.g., to quickly react to sudden power demand changes due to external disturbances. Multiple power sources also increase redundancy and safety as well as operability in heavy sea conditions. Moreover, electric drive could be used in emission restriction areas, such as, harbors, to obtain zero emissions. Currently hybrid-powered ships can reduce fuel consumption by 15–25%, when comparing to equivalent diesel-powered ships. Hybrid vessels are considered to be a way to eventually decarbonize shipping [1]–[3]. A basic illustration of a hybrid vessel single-line diagram can be seen in Figure 1.

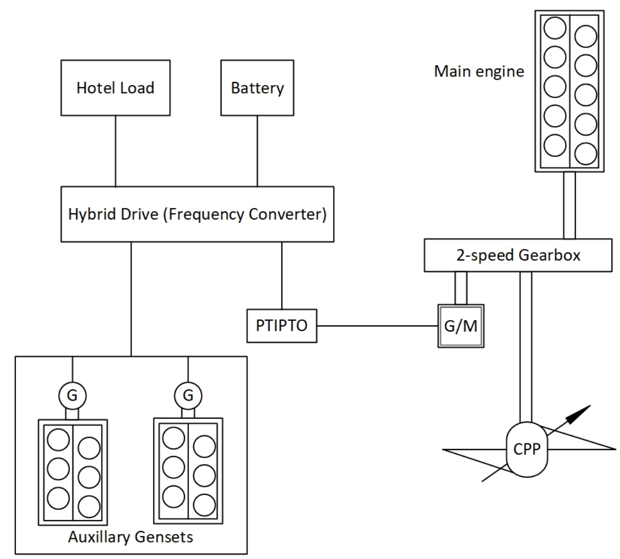

Fig. 1. Single line diagram of a hybrid vessel.

A typical hybrid vessel requires a hybrid cycle power system comprising the main engine (e.g. 4L20), lithium ion (Li-ion) battery arrays, battery management system (BESS), auxillary engines (or small Gensets), PTIPTO unit, the propeller (CPP), the frequency converter, the gearbox, and the other electrical load (also known as hotel load) [4]–[6].

The hybrid drive (controller) needs to know the state-of-charge (SoC) of the battery for energy management, safety, and proactive battery health monitoring [7]. As for energy management and efficiency, Estrada et al. [8] optimized the PTIPTO controller with Q-learning – a reinforcement learning algorithm. In the controller, the battery SoC, vehicle speed, and power demand were inputs. The output is the torque demand distribution between the internal combustion engine and the electric motor. The controller reduced fuel consumption by 23% in comparison to a non-hybrid vehicle.

B. Battery state of charge

SoC is used to select the operation mode of the hybrid system. With a low SoC (e.g., below 30%) the preferences should be to save the charge for emergencies and to charge the battery, whereas a higher SoC allows to optimize other objectives, such as, emissions and fuel efficiency [9].

As for safety, SoC estimation is needed to protect against overcharging, over-discharging, and overheating. Furthermore, SoC is vital when monitoring battery performance and prolonging the battery life. This can be achieved, e.g., by calculating the state of health (SOH) as the ratio of the maximal actual capacity to the rated capacity. This ratio tends to decrease when the battery ages [7], [10].

C. Methods of SoC estimation

SoC is defined as the ratio of the available quantities of charge $Q(t)$ when the battery is fully charged to the nominal capacity of the battery Q_n, as described in Equation (1).

$$SoC(t) = \frac{Q(t)}{Q_n}. \tag{1}$$

The nominal capacity Q_n is the maximum quantity of charge the battery can contain, defined by the battery manufacturer [11], [12].

The SoC value is not deterministic due to the uncertainty associated with its measuring environment; hence, it is estimated. The literature contains various classifications for battery SoC estimation methods. The simplest classification of SoC estimation methods divides them to direct and indirect methods [11], [12]. A list of battery SoC estimation methods is shown in Table I, adapted from [12].

One indirect method measures the open circuit voltage (OCV) of the battery. Figure 2 shows the OCV-SoC relation given the measured battery data from our Li-ion cells against the fitted curve using polynomial fitting. The key insight from this graph is that the relation between the voltage and SoC is noise at most SoC levels, while nonlinear with low SoC levels. These facts highlight the challenges of the SoC estimation.

TABLE I
STATE OF CHARGE ESTIMATION METHODS

Direct methods	Indirect methods
1) Coulomb counting (CC) 2) Open circuit voltage (OCV) 3) Electrochemical impedance spectroscopy (EIS)	* Model-Based methods 1) Equivalent circuit model (ECM) 2) Electrochemical model (EChM) * Adaptive filter-based methods 1) Kalman filters KF/EKF/UKF 2) Recursive least squares (RLS) 3) H-infinity filter (HIF) * Adaptive artificial intelligence based methods 1) Artificial neural networks (ANN) 2) Genetic algorithms (GA)

The objective of this paper is to apply a lightweight robust estimation method as the Kalman filtering to act as the main predictive algorithm for the Li-ion battery SoC estimation. Since the given system is nonlinear, we study and compare two denominations of Kalman filters capable to track the states of nonlinear systems: 1) Extented Kalman filter (EKF) and 2) Unscented Kalman filter (UKF). This objective was aligned as part of the Integrated Energy Solutions to Smart and Green Shipping (INTENS) project, conducted between the years 2018–2020 in Finland [13].

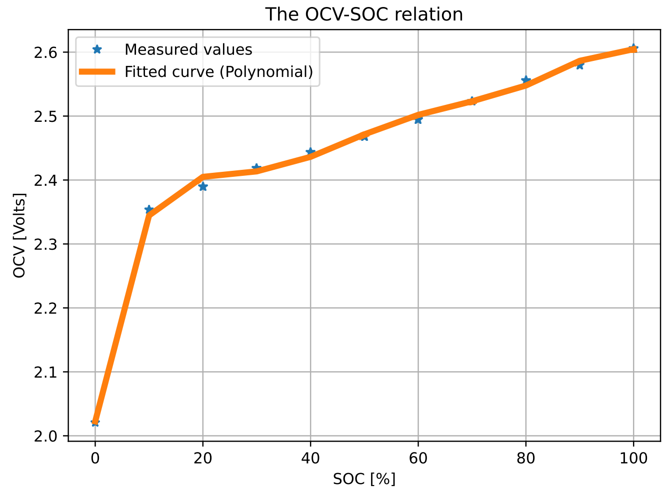

Fig. 2. Relation between battery open-circuit voltage and its state of charge. Note that the y-axis does not start from 0.

The rest of paper proceeds as follows: Section II discusses the technical aspects surrounding the adopted battery SoC estimation methodology, focusing on battery system modeling in the form of state-space set of equations. Section III shows the conducted simulations, their setup, and their respective results, graphically and numerically. Finally, Section IV concludes the paper by highlighting the key findings and insights from the applied method and the rendered results.

II. LI-ION BATTERY MODELING

Starting from battery system modeling, the operation of a given Li-ion battery can be projected via several ways, known as the equivalent circuit models (ECMs).

A. Equivalent circuit model

Numerous equivalent circuit models have been developed to best describe the behavior of Li-ion battery parameters and chemical activity. Examples are the Rint model, the RC model, Thevenin model, Dual polarization (DP) model and Partnership for a New Generation of Vehicles (PNGV) model, which are widely adopted in electric vehicles (EV) nowadays [14].

The DP model, shown in Figure 3, is an improved version of the Thevenin circuit model to express the polarization properties of the battery in a more refined manner [10]. The DP model consists of two RC elements to overcome the polarization simulation inaccuracy found in Thevenin, Rint and RC models. The DP model introduces two more factors than the Thevenin model, which are the concentration polarization and the electrochemical polarization [14]. The terminal voltage of the DP model is obtained from Equation (2) [10], [14].

$$U_{T,k} = U_{OC,k}\, SoC_k - U_{1,k} - U_{2,k} - R_{0,k}\, I_{T,k} + v_k \quad (2)$$

where $U_{T,k}$ is the circuit terminal voltage in Volts at time instant k, $U_{OC,k}$ is the open circuit voltage, SoC_k is the state of charge in percentage $\%$, $U_{1,k}$ is the voltage across the first RC branch, $U_{2,k}$ is the voltage across the second RC branch, $I_{T,k}$ is the circuit current flowing across its terminals in Amperes, and v_k is the error residual vector.

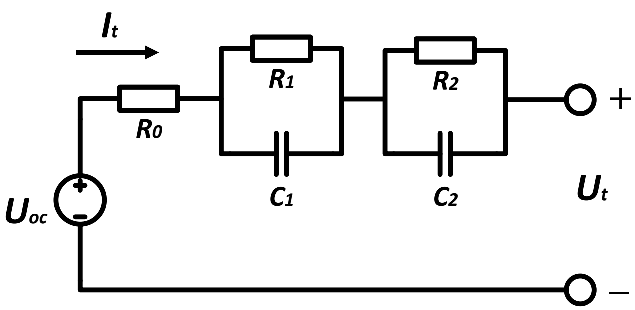

Fig. 3. Second order Thevenin circuit (or DP) model.

The relation between OCV U_{OC} and SoC can be derived mathematically as in [11], [15], [16], explained by Equation (3), and previously presented in Figure 2.

$$U_{OC}(SoC) = c_0 + c_1 S + c_2 S^2 + c_3 S^3 .. + c_n S^n . \quad (3)$$

where n is the polynomial order of the fitting function, and S is the function parameter to resemble the SoC estimation tensor.

Note that for computational optimization and accurate results in OCV-SoC relation, the recommended ceil of polynomial fitting order should be kept below the fifth order, as prescribed and implemented in [16]. While in our implementations, we discovered that the sixth-order polynomial fitting yielded more accurate results in both OCV-SoC relation and battery ECM parameter estimations.

B. Battery ECM parameters

According to the DP model, the following battery ECM parameters should be evaluated or estimated in order to facilitate SoC estimation, they are: $R_0, R_1, R_2, \tau_1, \tau_2, C_1, C_2$.

The evaluation of resistance parameters (R_0, R_1, R_2) and time constants (τ_1, τ_2) is performed according to the methodology described in Figure 4, as stated by [17], [18]. The method requires the determination of five turning points from the terminal voltage curves, as shown in Figure 4. In our study, the five turning points were detected by a Python-based script that was developed to pinpoint the triggered major changes (turning points) in the characteristic terminal voltage curves, based on the recorded experimental Li-ion battery data. Those points were arbitrary termed as: 1) Start point, 2) Falling point, 3) Stop point, 4) Rising point, and 5) Discharge point.

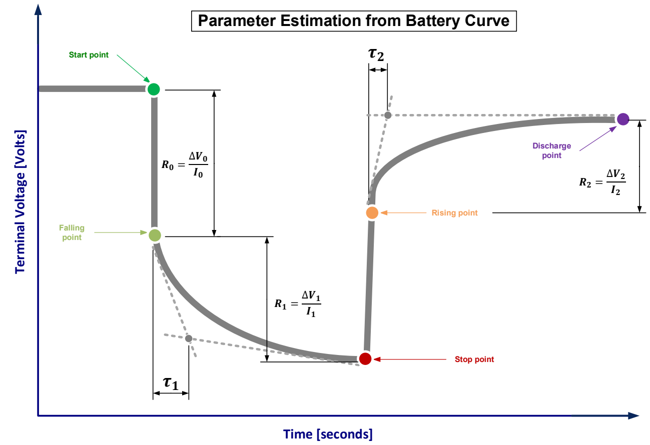

Fig. 4. Evaluating battery parameters from U_T curve data using the indicated formulas from [17], [18].

While current I_T flowing, the estimation of battery model ECM parameters $(U_1, U_2, R_1, R_2, C_1, C_2)$ are obtained via the hybrid pulse power characterization (HPPC) tests, as described in [10]. In the method, the offline battery curves are fitted using 6th-order polynomial curve-fit technique, as seen in Figure 5.

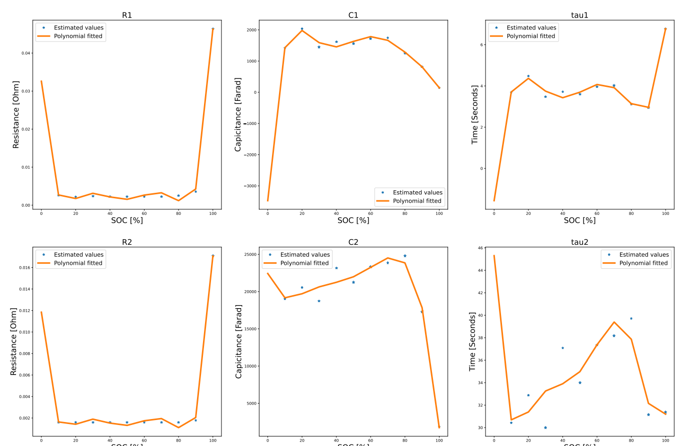

Fig. 5. ECM parameters fitted using sixth-order polynomial fitting model.

C. Kalman filters for battery SoC estimation

The Kalman filter is a recursive algorithm designed to iteratively estimate the optimal states of linear systems in the presence of additive white Gaussian noise [19]. The method employs the priori knowledge of the system to update the posterior state by calculating the Kalman gain and measurements residual, addressing errors due to drifts and mismatches. Then, it determines the updated state and covariance vectors, which serve as inputs for the subsequent iteration [20]–[22].

In discrete-time applications, the Kalman filter operates in two main steps, the prediction and update steps. In the **Prediction** step, the system's next state is forecasted using prior measurements. While in **Update** step, the current state is refined based on the most recent measurement. These steps correspond to state-space equations, as detailed in [21], [23].

The simplest form of the nonlinear state-space estimation model is expressed by Equations (4) [21].

$$\begin{aligned} x_k &= f(x_{k-1}) + q_{k-1}, \\ y_k &= h(x_k) + r_k. \end{aligned} \tag{4}$$

Where x_k denotes the state vector at time instant k, y_k represents the measurement vector, q_{k-1} and r_k denote the process and measurement noise vectors, respectively. These noise terms are assumed to follow normal distributions, with $q_{k-1} \sim N(0, Q_{k-1})$ and $r_k \sim N(0, R_k)$. The functions $f(.)$ and $h(.)$ express the nonlinear dynamics of the system and the measurement model, respectively.

Hence, according to the previous equations and formulas, the nonlinear Kalman state vector for Li-ion battery DP model can be written as in Equations (5).

$$\begin{aligned} x_k &= [SoC_k \;\; U_{1,k} \;\; U_{2,k} \;\; R_{0,k} \;\; R_{1,k} \;\; R_{2,k} \;\; C_{1,k} \;\; C_{2,k}]^T, \\ y_k &= [U_{1,k} \;\; U_{2,k} \;\; R_{0,k}]^T. \end{aligned} \tag{5}$$

Kalman transition equations of state and measurements vectors can be described by Equations (6): [10], [16]

$$\begin{aligned} SoC_{k+1} &= SoC_k - (\frac{\eta \Delta t}{Q_n})\, I_{T,k}, \\ U_{1,k+1} &= (e^{\frac{-\Delta t}{\tau_1}})\, U_{1,k} + R_{1,k}(1 - e^{\frac{-\Delta t}{\tau_1}}) I_{T,k}, \\ U_{2,k+1} &= (e^{\frac{-\Delta t}{\tau_2}})\, U_{2,k} + R_{2,k}(1 - e^{\frac{-\Delta t}{\tau_2}}) I_{T,k}, \\ R_{0,k+1} &= (c_1 + 2c_2 S_k + 3c_3 S_k^2)(S_k - \frac{\eta \Delta t}{Q_n})\, I_{T,k}. \end{aligned} \tag{6}$$

where SoC_k is the unit-less SoC value at time instant k in percentage %, η is the charge or discharge efficiency, Δt is the time step in seconds, Q_n is the maximum available capacity of the battery (the cell capacity), $I_{T,k}$ is the terminal current intensity across the circuit at time instant k in amperes, τ_1 and τ_2 are the constant time coefficients of the first and second RC branches, respectively, $U_{1,k}$ and $U_{2,k}$ are the voltage across the first and second RC branch at time instant k in volts, respectively, $c_1..c_3$ and S_k are the polynomial coefficients and the parametric tensor of R_0, respectively.

The extended Kalman filter (EKF) uses Taylor series approximation to linearize the joint distributions tangential point at each state estimation, as it assumes multivariate normal distribution [21], [22].

EKF extends the linear Kalman filter to suit nonlinear systems by approximating the joint distribution of state predictions and measurements as Gaussian spaces, centered around their mean value. This approximation is done by means of the Jacobian matrix and Taylor series approximation up to the first and second orders, such that the new state-space formulas can be re-written as shown in Equations (7) [10], [15], [16].

$$\begin{aligned} x_{k+1} &= A_k\, x_k + B_k\, u_k + w_k \\ y_{k+1} &= C_k\, x_k + D_k\, u_k + v_k \\ A_k &= \frac{\partial f(x_k, u_k)}{\partial x_k}, \quad B_k = \frac{\partial f(x_k, u_k)}{\partial u_k}, \\ C_k &= \frac{\partial h(x_k, u_k)}{\partial x_k}, \quad D_k = \frac{\partial h(x_k, u_k)}{\partial u_k}. \end{aligned} \tag{7}$$

The unscented Kalman filter (UKF) is another form of nonlinear Kalman estimators that differs from EKF. UKF proceeds by the transformation of a non-Gaussian distribution to a Gaussian one through nonlinear functions or spaces. Contrary to EKF, UKF utilizes multiple points including the mean of the distribution called sigma-points, whereas the EKF relies solely on the mean for its approximation. The UKF generates additional sigma points, along with the mean, to achieve a more accurate transformation [24]. This process, referred to as the Unscented Transform (UT), eliminates the need for evaluating Jacobian or Hessian matrices, thereby reducing computational complexity and enhancing accuracy [25]. Consequently, the UKF often outperforms the EKF in highly nonlinear systems, while the EKF remains effective for systems with moderate nonlinearity.

The UKF algorithm uses the unscented transform to obtain a Gaussian approximation of nonlinear problems. The state-space equations are applied same as in Equation (4), with additional steps of calculating the nearby sigma points. The number of these points are enumerated by satisfying the formula $2n + 1$ with n as the preset scaling factor that determines the total number of sigma points, in this case $n = 2$ to gather five sigma points (including the mean point). The rest of UKF algorithm proceeds similar to EKF (i.e. prediction and update steps) as described in Equations (6) and (7).

D. SoC estimation method

Our proposed Li-ion battery SoC estimation method is outlined in Figure 6. We conducted the HPPC test to verify the SoC estimation method against the simulation results, at a given temperature of 298.15 Kelvin.

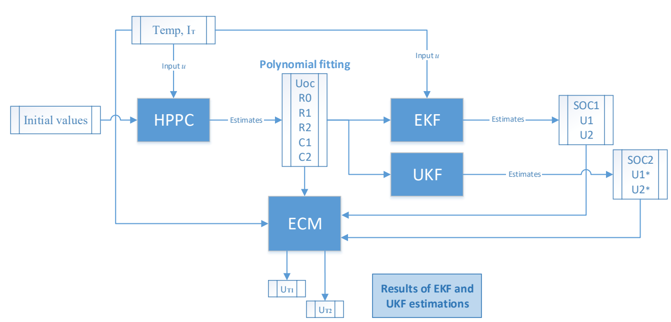

Fig. 6. Overview of the proposed Li-ion battery SoC estimation method.

The method commences with providing the initial guesses of HPPC parameters found from pre-recorded battery test data. Then, the output of the HPPC test influences the polynomial fitting of the battery ECM parameters, which in turn, are exported to the Kalman estimators EKF and UKF. A real-time ECM simulation model inbounds the estimated SoC values from the EKF/UKF output to evaluate the battery terminal voltage across the two RC branches.

III. Simulation and Results

Simulations were carried out in MATLAB R2021a, using a developed ECM model, built-in Simulink blocks for EKF/UKF estimators, and HPPC data inlets. Figure 7 shows the experimental terminal voltage of HPPC test, with zoomed-in posture in the below sub-plot.

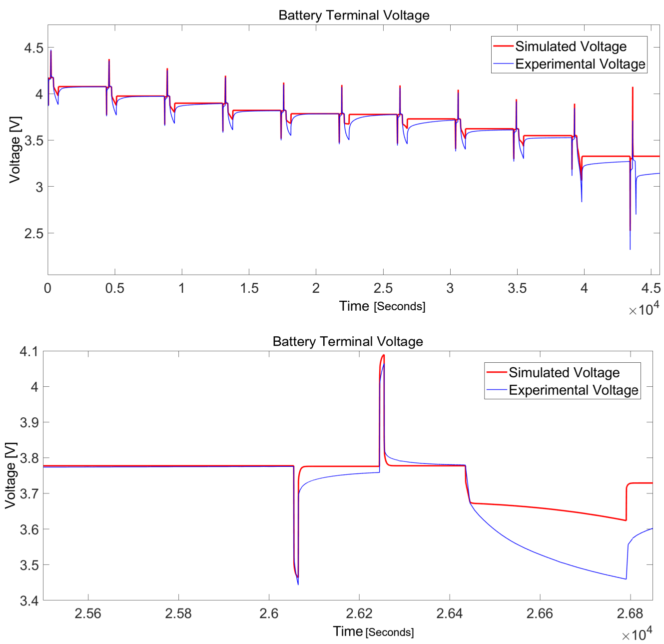

Fig. 7. Battery terminal voltage from HPPC test at 298.15 Kelvin.

The SoC simulation results are illustrated graphically in Figure 8, and numerically in Table II. The error residuals between EKF/UKF SoC and the reference SoC is shown in Figure 9.

The utilized performance metrics are: the mean absolute error (MAE), the root mean square error (RMSE), the 95th-percentile (p95%), and the statistical standard deviation and variance.

Based on the rendered results, it is evident that both EKF and UKF estimators are converging to SoC reference data from the HPPC test. However, UKF outperforms EKF in terms of estimation accuracy, as anticipated, with UKF-MAE = 0.05% against EKF-MAE = 0.11%.

TABLE II
Error Evaluation of EKF and UKF SoC Estimations

	MAE	RMSE	p95%	Std.	Var
EKF	0.11%	0.15%	0.35%	0.13%	0.013%
UKF	**0.05%**	**0.07%**	**0.10%**	**0.07%**	**0.017%**

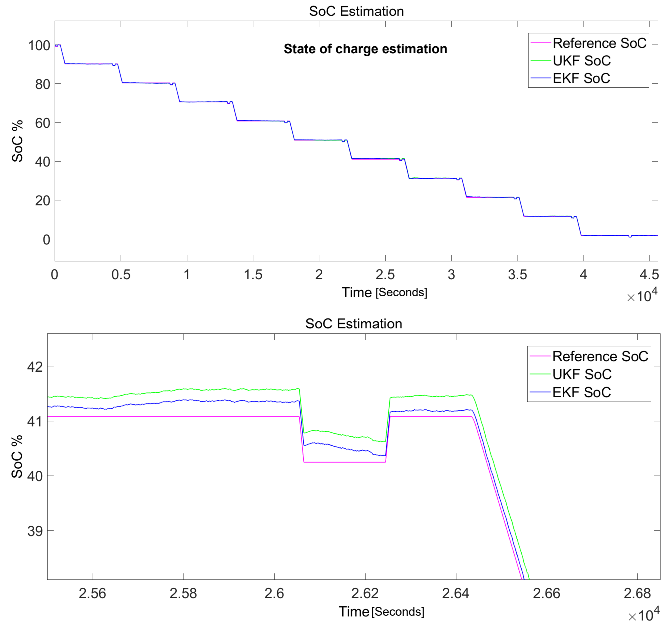

Fig. 8. Battery SoC estimation results using EKF/UKF.

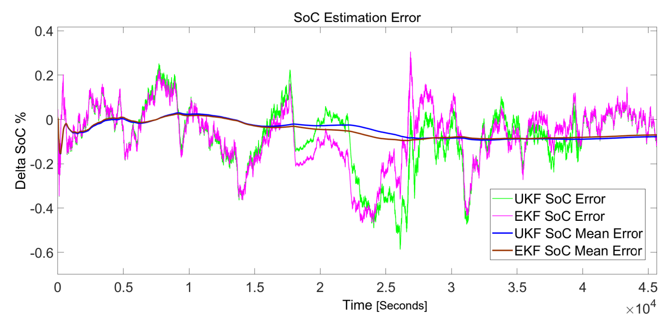

Fig. 9. SoC estimation errors of EKF/UKF compared to reference data.

IV. Conclusion

In this paper, we evaluated the performance of EKF and UKF predictive algorithms for estimating SoC in Li-ion batteries used in hybrid vessels. Our analysis was based on data from actual Nordic maritime operations and controlled laboratory tests, allowing to assess each filter's reliability under realistic operating conditions. Both the EKF and UKF showed steady SoC tracking capabilities, but differences emerged when comparing their performance across varying load demands. The results demonstrated that the UKF provided a more precise SoC estimate than the EKF, achieving a 0.05% improvement in accuracy. This enhanced accuracy was particularly evident during periods of rapid load changes, where UKF maintained a stable SoC estimate with minimal deviation, while EKF exhibited minor fluctuations. Such a performance edge makes the UKF better suited for real-time SoC monitoring, especially in maritime environments where power demands shift frequently and accurate battery management is critical to operational efficiency. These findings underscore the potential of Kalman filters in critical applications that demand responsive and accurate battery monitoring. Future studies could further validate these results with larger datasets and/or different experimental scenarios such as severe weather conditions or prolonged power fluctuations.

Acknowledgment

This work was carried out and supported by the INTENS project during the period of 2018–2020. Special thanks to the national collaborators: University of Vaasa, Wärtsilä Oy, VEBIC, and University of Lappeenranta.

References

[1] Z. Bei, J. Wang, Y. Li, H. Wang, M. Li, F. Qian, and W. Xu, "Challenges and Solutions of Ship Power System Electrification," *Energies*, vol. 17, no. 13, 2024.

[2] C. Sui, P. de Vos, D. Stapersma, K. Visser, and Y. Ding, "Fuel Consumption and Emissions of Ocean-Going Cargo Ship with Hybrid Propulsion and Different Fuels over Voyage," *Journal of Marine Science and Engineering*, vol. 8, no. 8, 2020.

[3] I. Skoko, T. Stanivuk, B. Franic, and D. Bozic, "Comparative Analysis of CO2 Emissions, Fuel Consumption, and Fuel Costs of Diesel and Hybrid Dredger Ship Engines," *Journal of Marine Science and Engineering*, vol. 12, no. 6, 2024.

[4] J. Koljonen, M. Elsanhoury, M. Elmusrati, and S. Niemi, "Advancing sustainable maritime with ai/ml enhanced hardware-in-the-loop testing," in *2024 International Workshop on Artificial Intelligence and Machine Learning for Energy Transformation (AIE)*, pp. 1–6, 2024.

[5] F. Gao, A. H. Brodtkorb, M. Zadeh, and S. M. Mo, "Power management and optimization of marine hybrid propulsion systems: A combinator surface methodology," *Ocean Engineering*, vol. 309, p. 118354, 2024.

[6] A. Thurman, "Hybrid ships: a surprising reason they are such an excellent idea."

[7] P. Dini, A. Colicelli, and S. Saponara, "Review on Modeling and SOC/SOH Estimation of Batteries for Automotive Applications," *Batteries*, vol. 10, no. 1, 2024.

[8] P. M. Estrada, D. d. Lima, P. H. Bauer, M. Mammetti, and J. C. Bruno, "Deep learning in the development of energy Management strategies of hybrid electric Vehicles: A hybrid modeling approach," *Applied Energy*, vol. 329, p. 120231, 2023.

[9] E. Choi and H. Kim, "Advanced Energy Management System for Generator–Battery Hybrid Power System in Ships: A Novel Approach with Optimal Control Algorithms," *Journal of Marine Science and Engineering*, vol. 12, no. 10, 2024.

[10] B. Nemounehkhah, R. Faranda, K. Akkala, H. Hafezi, C. Parthasarathy, and H. Laaksonen, "Comparison and Evaluation of State of Charge Estimation Methods for a Verified Battery Model," in *2020 International Conference on Smart Energy Systems and Technologies (SEST)*, pp. 1–6, 2020.

[11] W.-Y. Chang, "The State of Charge Estimating Methods for Battery: A Review," *International Scholarly Research Notices*, 2013.

[12] J. P. Rivera-Barrera, N. Muñoz-Galeano, and H. O. Sarmiento-Maldonado, "SoC Estimation for Lithium-ion Batteries: Review and Future Challenges," *Electronics*, vol. 6, no. 4, 2017.

[13] G. Zou, "Towards smart and green shipping | VTT News," May 2018.

[14] H. Hongwen, R. Xiong, and F. Jinxin, "Evaluation of Lithium-Ion Battery Equivalent Circuit Models for State of Charge Estimation by an Experimental Approach," *Energies*, 2011.

[15] Q. Yu, R. Xiong, C. Lin, W. Shen, and J. Deng, "Lithium-ion battery parameters and state-of-charge joint estimation based on h-infinity and unscented kalman filters," *IEEE Transactions on Vehicular Technology*, vol. 66, no. 10, pp. 8693–8701, 2017.

[16] M. A. Awadallah and B. Venkatesh, "Accuracy improvement of soc estimation in lithium-ion batteries," *Journal of energy storage*, vol. 6, pp. 95–104, 2016.

[17] B. Schweighofer, K. Raab, and G. Brasseur, "Modeling of high power automotive batteries by the use of an automated test system," *IEEE Transactions on Instrumentation and Measurement*, vol. 52, no. 4, pp. 1087–1091, 2003.

[18] D. Ali, S. Mukhopadhyay, H. Rehman, and A. Khurram, "Uas based li-ion battery model parameters estimation," *Control Engineering Practice*, vol. 66, pp. 126–145, 2017.

[19] R. E. Kalman, "A New Approach to Linear Filtering and Prediction Problems," *Journal of Basic Engineering*, vol. 82, pp. 35–45, mar 1960.

[20] F. A. Haugen, "State estimation with Kalman Filter," tech. rep., TechTeach, 2007.

[21] J. Hartikainen, A. Solin, and S. Särkkä, *Optimal filtering with Kalman filters and smoothers - a Manual for Matlab toolbox EKF/UKF*. Aalto University, 2011.

[22] R. Faragher, "Understanding the Basis of the Kalman Filter Via a Simple and Intuitive Derivation [Lecture Notes]," *IEEE Signal Processing Magazine*, vol. 29, pp. 128–132, sep 2012.

[23] Y. Bar-Shalom, "Recursive tracking algorithms: from the kalman filter to intelligent trackers for cluttered environment," in *Proceedings. ICCON IEEE International Conference on Control and Applications*, IEEE, 1989.

[24] S. Julier and J. Uhlmann, "Unscented Filtering and Nonlinear Estimation," *Proceedings of the IEEE*, vol. 92, pp. 401–422, mar 2004.

[25] S. Sarkka, "On Unscented Kalman Filtering for State Estimation of Continuous-Time Nonlinear Systems," *IEEE Transactions on Automatic Control*, vol. 52, pp. 1631–1641, sep 2007.